Electronic Supplementary Information (ESI) for Journal of Materials Chemistry A.
This journal is © The Royal Society of Chemistry 2021

Supporting Information

Reducing sputter induced stress and damage for efficient perovskite/silicon tandem solar cells

Kong Liu,[ab] Bo Chen,[*bc] Zhengshan J. Yu,[d] Yulin Wu,[a] Zhitao Huang,[a] Xiaohao Jia,[a] Chao Li,[a] Derrek Spronk,[c] Zhijie Wang,[a] Zhanguo Wang,[a] Shengchun Qu,[*a] Zachary C. Holman[*d] and Jinsong Huang[*bc]

[a.] Key Laboratory of Semiconductor Materials Science, Institute of Semiconductors, Chinese Academy of Sciences, Beijing, 100083, China. E-mail: qsc@semi.ac.cn

[b.] Department of Mechanical and Materials Engineering, University of Nebraska-Lincoln, Lincoln, NE 68588, USA.

[c.] Department of Applied Physical Sciences, University of North Carolina, Chapel Hill, NC 27599, USA. E-mail: jhuang@unc.edu, bochen@unc.edu

[d.] School of Electrical, Computer, and Energy Engineering, Arizona State University, Tempe, AZ 85287, USA. E-mail: Zachary.Holman@asu.edu

Materials and Methods

MD simulations

MD simulations were performed using the open source code Large Atomic/Molecular Massively Parallel Simulator (LAMMPS).[1] The Reax potential (ffield.reax.hns) was used to model molecular structures of BCP and C_{60}.[2] The interaction between the sputtered atoms and atoms in the molecule was estimated using L-J potential. A cutoff distance of 0.3 nm was employed for the interactions. The sputtering process was simulated by hitting a sputtered atom center-aligned towards the specific atoms in molecules with a preset velocity. Different atoms and angles have been tried to find the most likely generation of damage.

Perovskite solar cell preparation

Poly(triaryl amine) (PTAA, Sigma Aldrich) was dissolved in toluene with a concentration of 2 mg mL^{-1} and spin coated on ITO/glass substrates at a speed of 4000 rpm for 35 s. The spun films were then annealed at 100 °C for 10 min. $Cs_{0.15}(FA_{0.83}MA_{0.17})_{0.85}Pb(I_{1-x}Br_x)_3$ perovskite layers were fabricated by the antisolvent method. The pristine perovskite precursor solution was composed of mixed CsI, FAI, FABr, MAI, PbI_2, and $PbBr_2$ in the mixed solvent N, N-dimethylformamide (DMF): dimethyl sulfoxide (DMSO) = 2:1, v/v with a concentration of 1.35 M. In order to improve the wetting of the perovskite precursor solution on the PTAA film, the PTAA-coated ITO/glass substrate was pre-wetted by spinning DMF (50 μL) at 4000 rpm for 5 s. Then 80 μL of precursor solution was spun onto the PTAA at 2000 rpm for 2 s and 4000 rpm for 40 s, and the sample was quickly washed with toluene (130 μL) at the 35th second of the 4000 rpm spin coating process. Subsequently, the sample was annealed at 65 °C for 10 min and 100 °C for 15 min.

ICBA (Solaris Chem Inc.) solution in DCB with a concentration of 20 mg mL^{-1} was coated onto the perovskite surface at 6000 rpm for 35 s, and then annealed at 100 °C for 30 min. After that, C_{60} (20 nm) and BCP (8 nm) were evaporated on ICBA for the control devices. SnO_2 film was deposited by ALD with the following processing sequence: 0.5 s TDMASn pulse, 15 s

purge (20 sccm N_2), 0.1 s deionized water pulse, and 15 s purge (20 sccm N_2). The door and body temperature was maintained at 100 °C for the hot-wall reactor while the manifold temperature was 120 °C with a precursor temperature of 60 °C.[3] The Cu (80 nm) electrodes were prepared by thermal evaporation.

IZO film fabrication

The IZO films were prepared by RF magnetron sputtering with a 2-inch IZO (90 wt% In_2O_3 and 10 wt% ZnO) target. For IZO properties test, the films were fabricated on glass slide substrates. No intentional substrate heating was used. Before filling Ar/O_2, the chamber was set at a base pressure below 1×10^{-4} Pa. The working pressure of the chamber was set to 0.3 Pa by varying Ar/O_2 flow. The O_2/Ar ratio was set to 0.6%, which has been optimized as first step of our work based on the transmittance and conductivity of IZO film. Before deposition, a pre-sputtering process was operated for 5 min in order to clean the IZO target. The distance between the substrate and target can be varied from 5 cm to 20 cm. Unless otherwise specified, the source power of sputtering was set at 1.48 W/cm^2. Accordingly, the bias voltage between the target and substrate was 140 V. IZO film thickness was determined by controlling deposition time. For solar cell testing, the Cu fingers with a width of 130 μm and thickness of 300 nm were thermally evaporated on top of the IZO electrodes.

Perovskite/silicon tandem solar cell preparation

Our former paper has reported the process details of silicon bottom solar cell.[3] For perovskite top solar cells, the PTAA layer was spin coated on the silicon bottom cell at a speed of 4000 rpm for 35 s and then annealed at 100 °C for 10 min. Then the $Cs_{0.15}(FA_{0.83}MA_{0.17})_{0.85}Pb(I_{0.8}Br_{0.2})_3$ perovskite was used for absorber layer and the same spin-coating process in perovskite solar cell was performed. 20 mg·mL^{-1} ICBA solution in 1,2-dichlorobenzene was coated onto the perovskite surface at 6000 rpm for 35 s and then annealed at 100 °C for 30 min. Next, we thermally evaporated 20 nm of C_{60}. Then, 9 nm SnO_2 was deposited by ALD. 150 nm of IZO was sputtered on top of the SnO_2. The square cells are

defined as 6.5 mm × 6.5 mm through a shadow mask. 300-nm-thick Cu fingers with a width of 130 μm were thermally evaporated on top of the IZO layer. The effective area of cells is 40 mm^2 after deducting the area of Cu fingers. Finally, 150 nm of MgF_2 was thermally evaporated as an anti-reflection coating.

Characterization

Film thickness measurements were examined by using a Dektak XT Profiler. Transmission spectra of the films were measured by a PerkinElmer Lambda 950 spectrophotometer equipped with an integrating sphere. Glass slide was used as the baseline to get the neat transmittance of the IZO films. Sheet resistance measurements were taken by evaporating Cu pads onto the electrode surface to define a patterned square area, over which the resistance was measured using a multimeter.[4] Scanning electron micrographs (SEM) were taken with a Quanta 200 FEG environmental scanning electron microscope. For SEM sample preparing process, we used glass cutter to scribe a line with length about 1/4 of glass length at side with perovskite film, then broke the glass across the scribe line quickly. Glass and IZO are brittle enough to break quickly. No additional peeling-off of IZO was observed.

Current–voltage measurements were recorded using a Keithley 2400 Source-Measure Unit under simulated AM 1.5G irradiation (100 mW cm^{-2}), which was produced by a Xenon-lamp-based solar simulator (94043A, Newport Sol3A™ Class AAA). The light intensity was calibrated using a 91150-KG5 silicon reference cell and meter with a KG5 window. The stability tests were performed on device without encapsulation at around 55 ^oC in air. The data were collected at maximum power point per 10 min.

Thermal stress calculation

According to the thermal stress theory, the thermal stress in the film on a substrate could be described as:[5]

$$\sigma_f = \left(\frac{E}{1-\nu}\right)_f (\alpha_s - \alpha_f)(T - T_0) \quad (1)$$

Where σ_f is thermal stress in the film, E and v are the Young's modulus and Poisson's ratio of the film, α_s and α_f are the thermal expansion coefficient of the substrate and the film respectively, T and T_0 are the sample temperature and the room temperature respectively. Here in this work, film and substrate are IZO and BCP/C_{60}/perovskite, respectively. E and v of IZO are set to 141 GPa and 0.25 according to the literature.[6] The thermal expansion coefficient difference (α_s -α_f) between IZO and organic layers is assumed to a typical value 4×10^{-5} K^{-1}. When the sample is at a target-substrate distance of 8 cm and 10 cm (where severe IZO peeling-off will occur), the tested temperatures of samples are 77 ^{o}C and 54 ^{o}C, respectively. The room temperature is set to 300 K. Therefore, the thermal stress at 8 cm and 10 cm can be calculated to 330 MPa and 203 MPa according to Equation (1).

Supporting figures

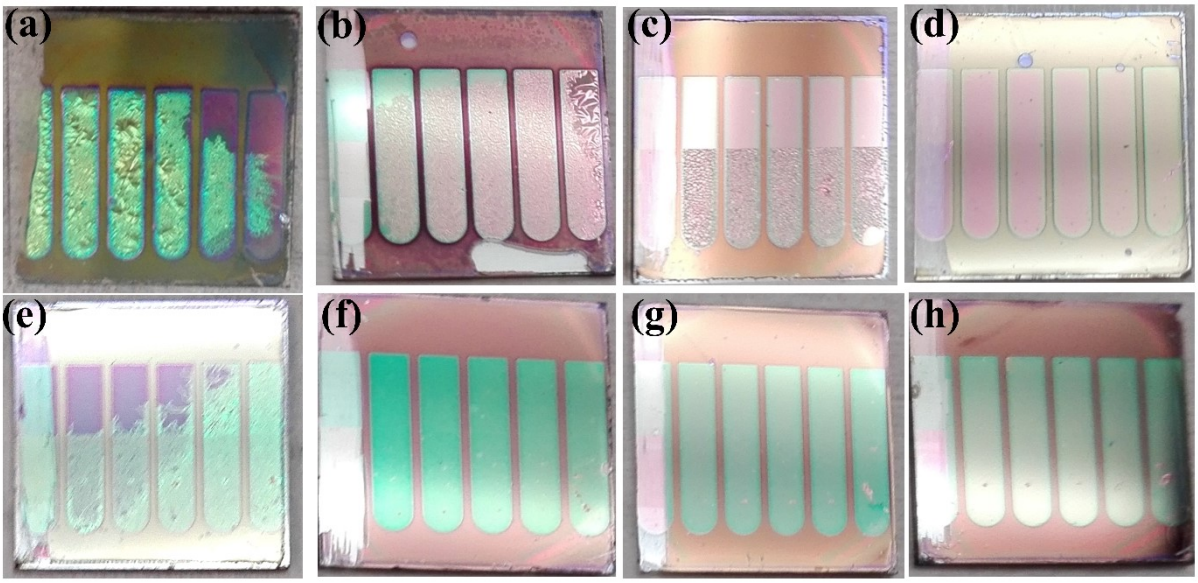

Fig. S1 Photograph of perovskite solar cells with BCP buffer layer and IZO electrodes deposited at a target-substrate distance of (a) 8 cm, (b) 10 cm, (c) 12 cm, and (d) 14 cm. Photograph of perovskite solar cells with SnO_2 buffer layer and IZO electrodes deposited at a target-substrate distance of (e) 8 cm, (f) 10 cm, (g) 12 cm, and (h) 14 cm.

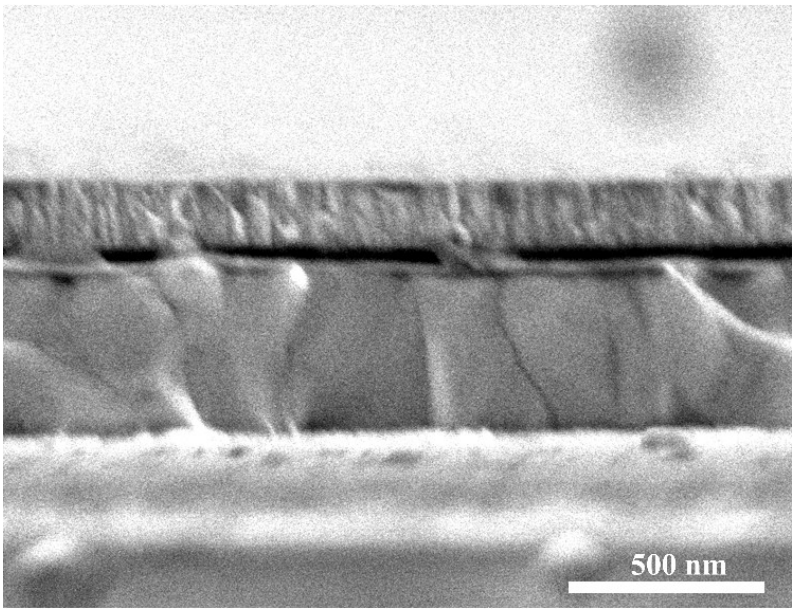

Fig. S2 Cross-section SEM image of a perovskite solar cell with SnO_2 buffer layer.

Fig. S3 Photograph of perovskite solar cells with SnO_2 buffer layer and IZO electrodes deposited at a target-substrate distance of 10 cm after cooling to -5 ^oC.

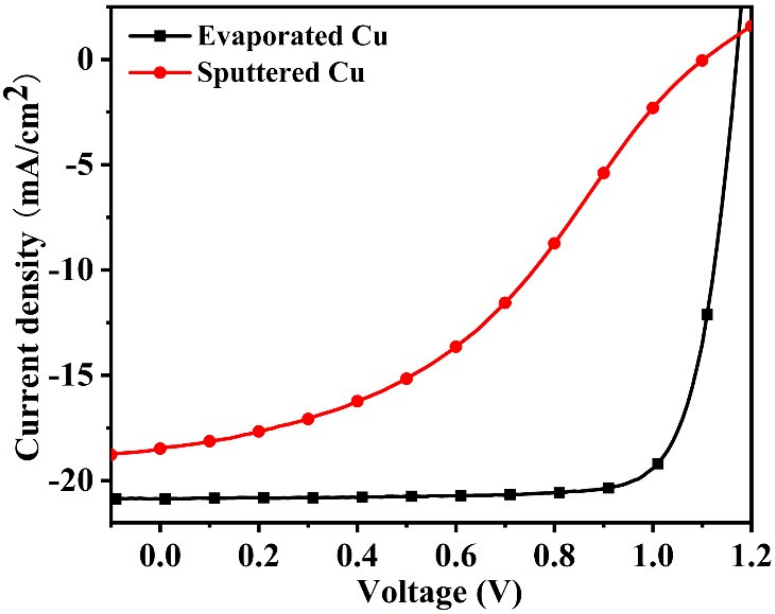

Fig. S4 *J-V* characteristics of the perovskite solar cells with evaporated Cu and sputtered Cu electrodes.

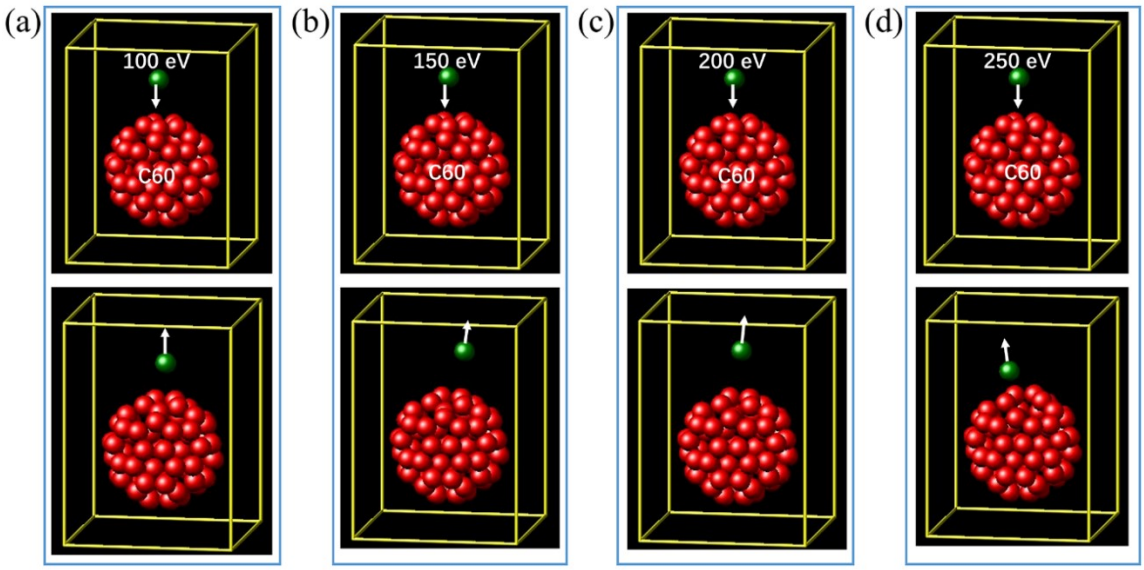

Fig. S5 MD simulations on collision between indium atom and C_{60} molecule. The kinetic energy of indium atoms were set to (a) 100 eV, (b) 150 eV, (c) 200 eV and (d) 250 eV.

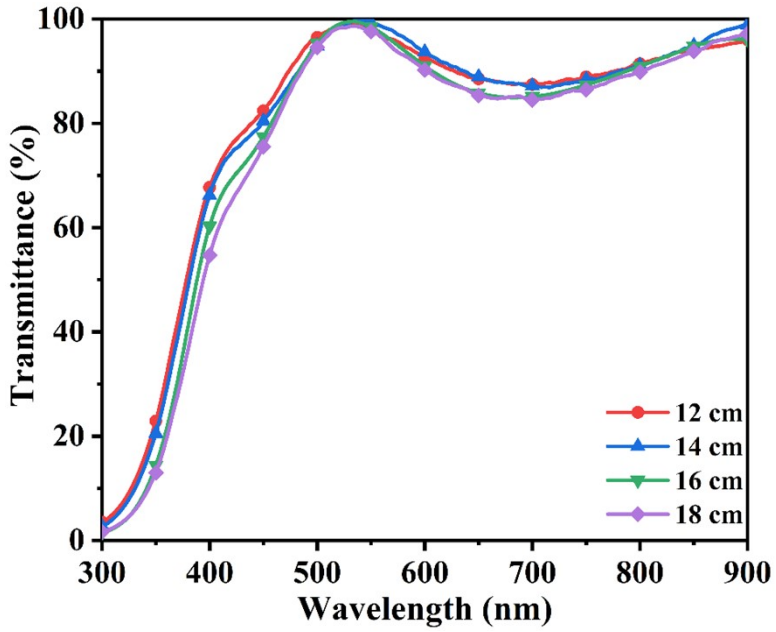

Fig. S6 Transmittance of IZO films (250 nm) deposited at target-substrate distance of 12 cm, 14 cm, 16 cm and 18 cm. The corresponding sheet resistance of the films are 16.4 Ω/sq, 17.6 Ω/sq, 24.6 Ω/sq and 30.7 Ω/sq for the target-substrate distance of 12 cm, 14 cm, 16 cm, and 18 cm, respectively.

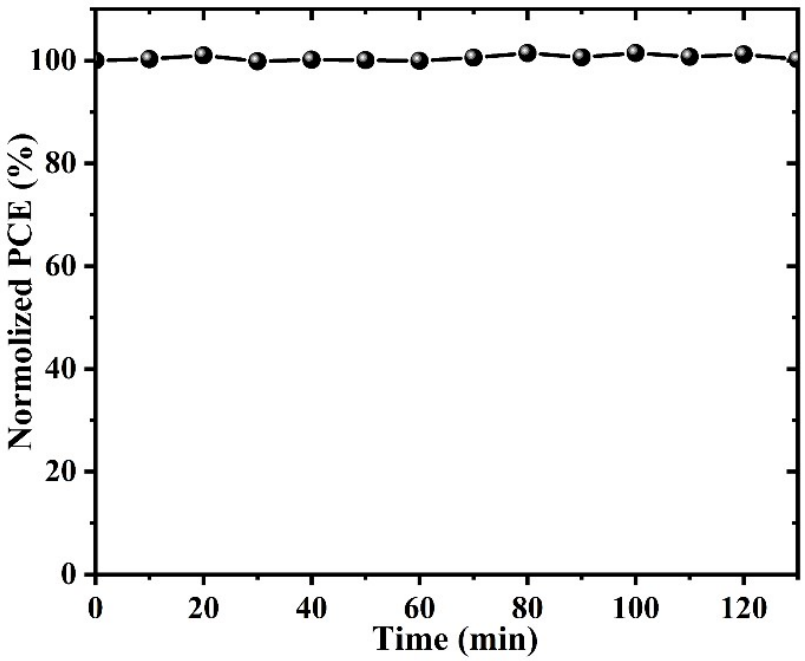

Fig. S7. *PCE* stability test of the tandem device without encapsulation under AM1.5G simulator sunlight at maximum power point at around 55 °C in ambient atmosphere.

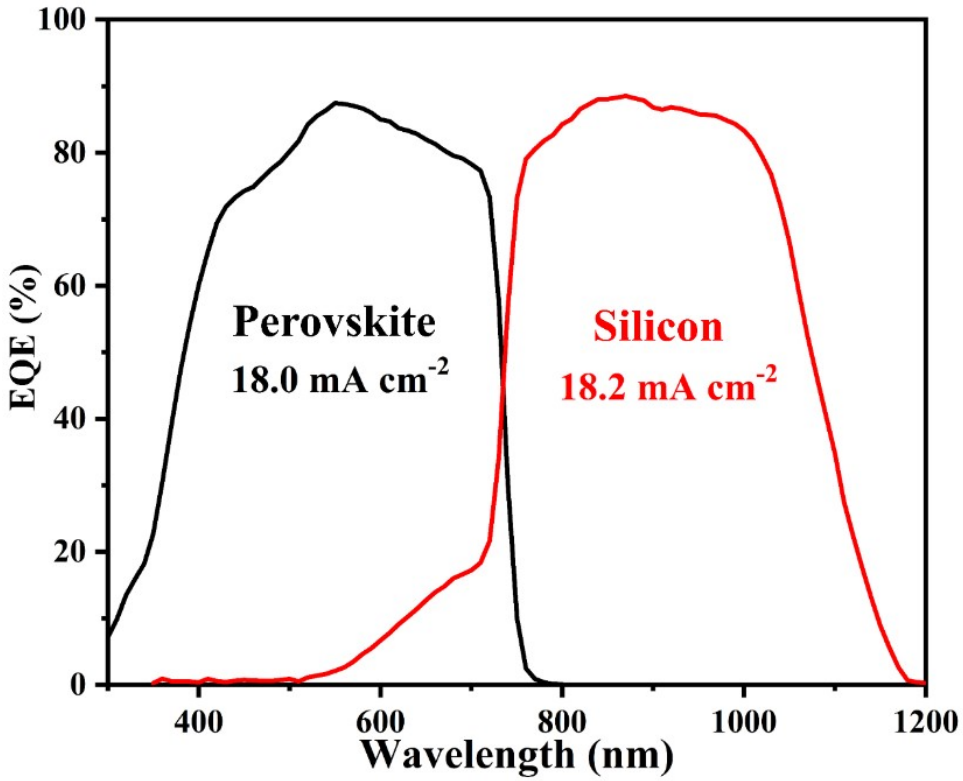

Fig. S8. EQE of perovskite/silicon tandem solar cell.

REFERENCES

1 S. Plimpton, *J. Comput. Phys.*, 1995, **117**, 1-19.
2 T. P. Senftle, S. Hong, M. M. Islam, S. B. Kylasa, Y. X. Zheng, Y. K. Shin, C. Junkermeier, R. Engel-Herbert, M. J. Janik, H. M. Aktulga, T. Verstraelen, A. Grama and A. C. T. van Duin, *NPJ Comput. Mater.*, 2016, **2**, 15011.
3 B. Chen, Z. Yu, K. Liu, X. Zheng, Y. Liu, J. Shi, D. Spronk, P. N. Rudd, Z. Holman and J. Huang, *Joule*, 2019, **3**, 177-190.
4 W. Gaynor, G. F. Burkhard, M. D. McGehee and P. Peumans, *Adv. Mater.*, 2011, **23**, 2905-2910.
5 E. B. T. Walch, A. Benedetto, J. Bacharouche and C. Roos, *Int. J. Appl. Glass Sci.*, 2020, **11**, 707-719.
6 K. Sim, Z. Rao, Z. Zou, F. Ershad, J. Lei, A. Thukral, J. Chen, Q.-A. Huang, J. Xiao and C. Yu, *Sci. Adv.*, 2019, **5**, eaav9653.